Journal of Biomolecular NMR **30:** 233–244, 2004.

Secondary structural effects on protein NMR chemical shifts

Yunjun Wang*
Mesolight, LLC, Fayetteville, AR 72704, U.S.A.

Received 18 March 2004; Accepted 12 August 2004

Key words: chemical shift prediction, NMR, protein chemical shift, secondary structural effects

Abstract

For an amino acid in protein, its chemical shift, $\delta(\phi, \psi)_s$, is expressed as a function of its backbone torsion angles (ϕ and ψ) and secondary state (s): $\delta(\phi, \psi)_s = \delta(\phi, \psi)_{coil} + \Delta\delta(\phi, \psi)_s$, where $\delta(\phi, \psi)_{coil}$ represents its chemical shift at coil state (s = coil); $\Delta\delta(\phi, \psi)_s$ (s = sheet or helix) is herein defined as secondary structural effect correction factor, which are quantitatively determined from Residue-specific Secondary Structure Shielding Surface (RSS) for ^{13}CO, $^{13}C\alpha$, $^{13}C\beta$, $^{1}H\alpha$, ^{15}N, and ^{1}HN nuclei. The secondary structural effect correction factors defined in this study differ from those in earlier investigations by separating out the backbone conformational effects. As a consequence, their magnitudes are significantly smaller than those earlier reported. The present $\Delta\delta(\phi, \psi)_{sheet}$ and $\Delta\delta(\phi, \psi)_{helix}$ were found varying little with backbone conformation and the 20 amino acids, specifically for ^{13}CO, $^{13}C\alpha$, and $^{1}H\alpha$ nuclei. This study also carries out some useful investigations on other chemical shift prediction approaches – the traditional shielding surfaces, SHIFTS, SHIFTX, PROSHIFT, and identifies some unexpected shortcomings with these methods. It provides some useful insights into understanding protein chemical shifts and suggests a new route to improving chemical shifts prediction. The RSS surfaces were incorporated into the program PRSI [Wang and Jardetzky, J. Biomol. NMR, 28: 327–340 (2004)], which is available for academic users at http://www.pronmr.com or by sending email to the author (yunjunwang@yahoo.com).

Introduction

NMR chemical shifts of amino acids in proteins may be the most sensitive and easily obtainable parameters that reflect the primary, secondary, and tertiary structure of the protein. The structural effects permit the identification of chemically identical, but positionally nonequivalent, amino acid residues and thus form the basis of all structure determination by nuclear magnetic resonance (NMR) (Roberts and Jardetzky, 1970). To date, the best-known and mostly studied structural effect is probably the secondary structural effects (Markley et al., 1967; Nakamura and Jardetzky, 1968; Spera and Bax, 1991; de Dios et al., 1993; Oldfield, 1995). Over past 20 years, the secondary structural effects have been investigated in a similar manner – through comparing the observed β-sheet or α-helix chemical shifts to that of coil (Szilagyi and Jardetzky, 1989; Spera and Bax, 1991; Wishart et al., 1991; Le and Oldfield, 1994; Osapay and Case, 1994; Oldfield, 1995; Wang and Jardetzky, 2002a, b). In this study, Residue-specific Secondary Structure (RSS) ϕ/ψ chemical shift shielding surfaces were constructed and used to investigate the β-sheet or α-helix induced effects on ^{13}CO, $^{13}C\alpha$, $^{13}C_\beta$, $^{1}H\alpha$, ^{15}N, and ^{1}HN chemical shifts of proteins. The difference of using RSS shielding surfaces to study the secondary structural effects in chemical shifts is in that the backbone conformational effects are removed. The results from this study show that the traditionally defined

*To whom correspondence should be addressed. E-mail: yunjunwang@yahoo.com

secondary structural effect can be decomposed into two components – backbone conformational effects and 'secondary structural effects' as defined in this study.

Understanding the origins of chemical shifts could lead to new ways of determining or refining protein structure (Wishart et al., 1992; Wishart and Sykes, 1994; Celda et al., 1995; Williamson et al., 1995; Beger and Bolton, 1997; Cornilescu et al., 1999). However, since there are so many parameters that might have influence on the observed chemical shifts, attempts to define individual contributions to the overall chemical shift and introduce appropriate correction factors have thus far been met with limited success. Over the past 10 years, the rapid accumulation of chemical shift and three dimensional structure databases has made it possible to begin investigating each individual contribution to the overall chemical shift. For example, in the past several years, the empirical chemical shift database has successfully allow the identification of the secondary structure effects (Wishart et al., 1991; de Dios et al., 1993, Wang and Jardetzky, 2002a), correlation of the chemical shift with backbone torsion angles (Spera and Bax, 1991; Le and Oldfield, 1994), the hydrogenbond and side-chain geometry effects (Iwadate et al., 1999), contributions of specific structural features, such as the helix capping box (Gronenborn and Clore, 1994) and β-hairpin (Santiveri et al., 2001), and the nearest neighboring effects (Wang and Jardetzky, 2002b). Consequently, these results were successfully used for chemical shift prediction and secondary structural identification (Wishart et al., 1992; Wishart and Sykes 1994; Kuszewski et al., 1995; Wang and Jardetzky, 2004). Therefore, the author believes that the new concept of secondary structural effects as proposed and determined in this study could provide useful insight into the understanding of protein chemical shifts and eventually find applicable use in secondary structure identification, tertiary structure determination, and structural refinement using chemical shifts. This study also demonstrated improved chemical shift prediction from 3D coordinates, specifically for α-helix random coil chemical shifts, by using RSS (XRSS) shielding surfaces.

Methods

Nomenclature and definition

For an amino acid in protein with restricted backbone torsion angles (ϕ and ψ) and a defined secondary structural type (s), its chemical shift, δ(ϕ, ψ), is expressed as

$$\delta(\phi,\psi)_s = \delta(\phi,\psi)_{coil} + \Delta\delta(\phi,\psi)_s, \quad (1)$$

where $\delta(\phi, \psi)_{coil}$ represents its chemical shift at random-coil state; $\Delta\delta(\phi, \psi)_s$ is herein defined as the secondary structural effect correction factor; s stands for the three secondary structural types, β-sheet, random-coil, and α-helix. By definition, $\Delta\delta(\phi, \psi)_s$ equals zero when s = coil. Torsion angle of the preceding residue, ψ^{i-1}, is used for ^{15}N and ^{1}HN nuclei through this study. It is also hereinafter referred to as ψ for simplicity.

Preparation of the chemical shift database

Assigned ^{3}CO, $^{13}C\alpha$, $^{13}C_\beta$, $^{1}H\alpha$, ^{15}N, and ^{1}HN chemical shifts were downloaded from BioMagResBank (BMRB; http://www.bmrb.wisc.edu) and those meeting the following criteria were selected. (1) The length of protein sequence is above 50, (2) The most commonly used materials, DSS, TMS, TSP, and liquid NH_3 were used as either direct or indirect ^{15}N, ^{13}C, and ^{1}H chemical shift references (Wishart et al., 1995). Paramagnetic proteins, which were identified through checking the 'paramagnetic' property as reported in each BMRB entry, were not included in the database. When several BMRB entries were available for the same protein, the priority was given to the one with the most complete assignments. Abnormal chemical shift assignments (many of them were found to be obvious typing errors, e.g., 8.7 ppm for a ^{15}N shift) were excluded. The assignments of the very first two N-terminal and last two C-terminal residues of each protein were also excluded to avoid any terminal effects on chemical shifts. The 3D coordinates of the selected protein were downloaded from the Protein Data Bank (http://www.rcsb.org/pdb), from which torsion angles (ϕ, ψ and χ^1) as well as the secondary structural type were determined by using the program VADAR (Willard et al., 2003). This structural information was then combined with assigned chemical shifts to form a chemical shift-structure

database, which contains ^{13}CO, $^{13}C\alpha$, $^{13}C_\beta$, $^{1}H\alpha$, ^{15}N, and ^{1}HN chemical shift assignments derived from 467 distinct non-paramagnetic proteins. The BMRB and PDB accession numbers of the selected proteins are listed in the supplementary materials. Each entry in the database contains the assigned chemical shift, torsion angles (ϕ, ψ and χ^1), and secondary structural type. In addition, a unique ID was assigned to each entry to trace its origin. For an example, ID bmr4834_50 represents that this entry is originally derived from protein with BMRB access number of 4834 and the residue number is 50.

Non-RSS, RSS, and XRSS shielding surface

For each nucleus, the prepared chemical shift database was split into 20 subsets based on the amino acid type of the target residue to form the traditional residue specific database. In comparison with present RSS and XRSS, these traditional residue specific databases are purported as non-RSS through this study. For each of the 20 amino acids, above prepared residue specific database was further split into three subsets – RSS database based on the three secondary structural types – sheet, coil, and helix. For amino acids Val, Ile, Thr, Phe, His, Tyr, and Trp, each RSS database was further split into three χ^1 specific subsets (XRSS), where $\chi^1 = 180 - 30°$ or $-180 + 30°$ (hereinafter referred to as $180 \pm 30°$), $60 \pm 30°$, or $-60 \pm 30°$. Two subset databases were also built for Cys based on its $^{13}C_\beta$ shift adjusted re-oxidation states. Except for those amino acids with low occurrence such as Cys and Trp, there were excess chemical shift entries in most of RSS database. When applicable, the number of chemical shift entries was randomly trimmed to 500.

The chemical shift is calculated by convoluting each of the chemical shift values in selected database with a Gaussian function as suggested by Le and Oldfield (1994):

$$\delta(\phi,\psi) = \frac{\sum_i \delta(\phi_i,\psi_i) * \exp\left\{-\left[\sin^2\left(\frac{\phi_i-\phi}{2}\right) + \sin^2\left(\frac{\psi_i-\psi}{2}\right)\right]/A\right\}}{\sum_i \exp\left\{-\left[\sin^2\left(\frac{\phi_i-\psi_i}{2}\right)\sin^2\left(\frac{\psi_i-\psi}{2}\right)\right]/A\right\}},$$

where A is a constant and is set to 0.03 unless otherwise indicated, and the summations extend over all residues i in the corresponding database. During the calculation, when a given chemical shift was computed, that shift itself was identified via its specifically assigned ID and was excluded during the convoluting calculation.

Adjustment for ^{15}N and ^{13}C chemical shift references

Improper ^{15}N and ^{13}C chemical shift referencing is one of the problems associated with the protein chemical shift assignments deposited in BMRB (Iwadate et al., 1999; Wishart and Case, 2001). It has been shown by Zhang et al that a significant amount (~25%) BMRB entries with protein ^{15}N and ^{13}C chemical shift assignments required significant (>1.0 ppm) reference readjustments (Zhang et al., 2003). In this study, ^{13}C and ^{15}N chemical shift reference was carefully checked for each protein. Reference readjustments were made accordingly using the protocols which is similar to that used by Zhang et al. (2003). More specifically, the ^{13}CO, $^{13}C\alpha$, $^{13}C\beta$, $^{1}H\alpha$, ^{15}N and ^{1}HN chemical shifts were predicted from the torsion angles (ϕ, ψ and χ^1) using RSS and XRSS (for amino acids Val, Ile, Thr, Phe, His, Tyr, and Trp) shielding surfaces for each protein. The ^{13}C, ^{15}N and ^{1}H chemical shift reference offsets were determined by averaging the difference between the observed and the predicted chemical shifts for each protein. As an external check, the reference offsets calculated in this study were thoroughly compared with those reported by Zhang et al. (2003). The two sets of reference offset were found in a good agreement for more than 200 proteins that are exclusively included in both databases. The averaged differences between the two sets of reference offsets are less than 0.5 ppm and 0.15 ppm for ^{15}N and ^{13}C shifts – that is statistically insignificant for these two nuclei in proteins. The correlation coefficients between the two sets of data are 0.93 and 0.97; rmsd 0.31 and 0.16 ppm for ^{15}N and ^{13}C shifts. The ^{15}N and ^{13}C reference adjustments were made for each entry in non-RSS and RSS database. No significant reference offsets (e.g., >0.05 ppm) were identified for $^{1}H\alpha$ and ^{1}HN shifts for most of the proteins. Accordingly, no reference adjustments were made for these two nuclei.

Determination of $\langle \Delta\delta(\phi,\psi)n,s\rangle$

The secondary structural effect correction factor, $\Delta\delta(\phi, \psi)_s$, can be determined from Equation 1. For example, the β-sheet induced effect is calculated by:

$$\Delta\delta(\phi,\psi)_{\text{sheet}} = \delta(\phi,\psi)_{\text{sheet}} - \delta(\phi,\psi)_{\text{coil}},$$

where $\delta(\phi, \psi)_{\text{sheet}}$ and $\delta(\phi, \psi)_{\text{coil}}$ are calculated from sheet and coil specific RSS (or XRSS for Val, Ile, Thr, Phe, His, Tyr, and Trp) shielding surfaces, respectively. The α-helix induced effect is calculated in a similar way. As it will be described later, $\delta(\phi, \psi)_{\text{sheet}}$ and $\delta(\phi, \psi)_{\text{coil}}$ were found to vary little with the backbone dihedral angles (ϕ and ψ). Therefore, the average of $\Delta\delta(\phi, \psi)_s$ over the sheet and helix backbone conformational space (ϕ, ψ), defined as $\langle\Delta\delta(\phi,\psi)_{\text{sheet}}\rangle$ and $\langle\Delta\delta(\phi,\psi)_{\text{helix}}\rangle$, were calculated and used to generally represent the secondary structural effects on ^{13}CO, $^{13}C\alpha$, $^{13}C_\beta$, $^{1}H\alpha$, ^{15}N, and ^{1}HN chemical shifts in proteins. More specifically, for example, $\Delta\delta(\phi, \psi)_{\text{sheet}}$ was calculated and averaged at a 5-degree interval of ϕ and ψ over the β-sheet conformational space as defined in this study (−50–−180° and 80–180° for ϕ and ψ, respectively).

Determination of $\Delta\delta^{\text{pre-obs}}$

In this study, the mathematic difference between the predicted and the observed chemical shift is denoted as $\Delta\delta^{\text{pre-obs}}$.

$$\Delta\delta^{\text{pre-obs}} = \delta^{\text{pred}} - \delta^{\text{obs}}.$$

To evaluate the influence of the secondary structural effects on chemical shift prediction, the random coil status was further split into two subclasses, β-sheet like and α-helix like coils, representing those with ϕ and ψ in β-sheet and a-helix region, respectively. In this study, β-sheet like coil is marked as c_sheet; α-helix like coil c_helix. Thus, when applicable, the status of an amino acid in protein was categorized into four groups: sheet, c_sheet, c_helix, and helix, representing the β-sheet, β-sheet like coil, α-helix like coil, and α-helix. Respectively, the $\Delta\delta^{\text{pre-obs}}$ calculated for these four groups are marked as $\Delta\delta^{\text{pre-obs}}$ (sheet), $\Delta\delta^{\text{pre-obs}}$ (c_sheet), $\Delta\delta^{\text{pre-obs}}$ (c_helix), and $\Delta\delta^{\text{pre-obs}}$ (helix).

The β-sheet ϕ and ψ conformational region is defined as −50 to −180° and 80–180°; and that for helix −40 to −70° and −10 to−70°.

The chemical shift predicted from non-RSS shielding surfaces is solely dependent on its ϕ and ψ. For example, for an amino acid with its ϕ and ψ in the β-sheet region, regardless of its secondary structural status (either random coil or β-sheet), its chemical shifts predicted from non-RSS is simply a weighted average of the chemical shifts of all the amino acids in that region.

$$\delta^{\text{non-RSS}} = \frac{(N_{\text{c\_sheet}}{}^{*}\delta_{\text{c\_sheet}} + N_{\text{sheet}}{}^{*}\delta_{\text{sheet}})}{(N_{\text{c\_sheet}} + N_{\text{sheet}})}, \tag{2}$$

where $\delta_{\text{c\_sheet}}$ and $N_{\text{c\_sheet}}$ are the averaged chemical shifts and number of β-sheet like coil in the database; δ_{sheet} and N_{sheet} are the averaged shifts and number of β-sheet shifts. Ignoring the ϕ and ψ, equation 1 can be expressed as:

$$\delta_{\text{sheet}} = \delta_{\text{c\_sheet}} + \Delta\delta_{\text{sheet}}, \tag{3}$$

where $\delta_{\text{c\_sheet}}$ represents the β-sheet like random-coil chemical shifts, and $\Delta\delta_{\text{sheet}}$ is the β-sheet induced effect correction factor. Combination of Equations 2 and 3 results in the following:

$$\Delta\delta^{\text{pre-obs}}(\text{sheet}) = \delta^{\text{non-RSS}} - \delta_{\text{sheet}} = \frac{-\Delta\delta_{\text{sheet}}{}^{*}N_{\text{c\_sheet}}}{(N_{\text{c\_sheet}} + N_{\text{sheet}})}, \tag{4}$$

$$\Delta\delta^{\text{pre-obs}}(\text{c\_sheet}) = \delta^{\text{non-RSS}} - \delta_{\text{sheet}} = \frac{\Delta\delta_{\text{sheet}}{}^{*}N_{\text{c\_sheet}}}{\times/(N_{\text{c\_sheet}} + N_{\text{sheet}})}. \tag{5}$$

In a similar way:

$$\Delta\delta^{\text{pre-obs}}(\text{helix}) = \frac{-\Delta\delta_{\text{helix}}{}^{*}N_{\text{c\_helix}}}{(N_{\text{c\_helix}} + N_{\text{helix}})}, \tag{6}$$

$$\Delta\delta^{\text{pre-obs}}(\text{c\_helix}) = \frac{-\Delta\delta_{\text{helix}}{}^{*}N_{\text{\_helix}}}{(N_{\text{c\_helix}} + N_{\text{helix}})}, \tag{7}$$

where $N_{\text{c\_helix}}$ is the number of α-helix like random coil chemical shifts, and N_{helix} is the number of α-helix shifts in the database.

The number of chemical shifts for each of the four groups, N_{strand}, $N_{\text{c\_strand}}$, $N_{\text{c\_helix}}$, and N_{helix}

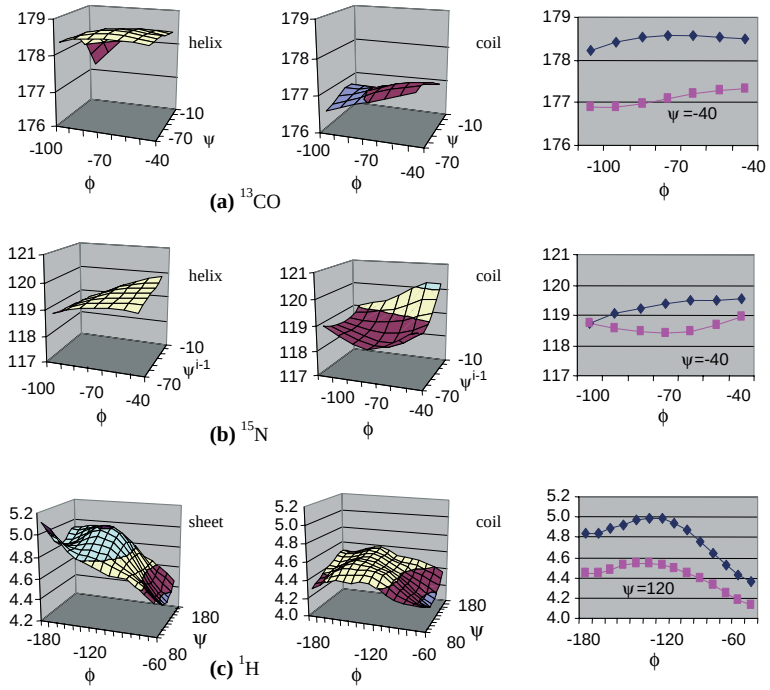

Figure 1. Representative RSS shielding surfaces show the variations of ^{13}CO (a), ^{15}N (b), and ^{1}Hα(c) chemical shifts of Lys with the secondary structural types and torsion angles, ϕ and is ψ On the left are helical and sheet specific RSS surfaces; on the middle are coil specific RSS surfaces. For comparison, slices from the left and middle figures are shown on the right.

were statistically determined from each corresponding database in this study.

All the calculations and data manipulations were accomplished using a series of JAVA programs coded by the author.

Results and discussion

RSS shielding surfaces

As an example, selected regions of ^{3}CO, ^{15}N, and ^{1}Hα RSS surfaces for one of the 20 amino acids, Lys, are shown in Figure 1. These RSS surfaces clearly demonstrate how ^{13}CO, ^{15}N, and ^{1}Hα chemical shifts vary with the secondary structural type as well as the backbone torsion angles,ϕ and ψ. On the left of this figure are the selected regions of helical and sheet RSS shielding surfaces, on the middle are the coil RSS surfaces. For a clear comparison, a slice from each of the helical (or sheet) and coil RSS surfaces are extracted and shown on the right. The helical RSS shielding surfaces differ significantly from the coil RSS surfaces by ~1.6 ppm, and 1.0 ppm for ^{13}CO and ^{15}N nuclei, respectively as shown in Figure 1a and 1b. While the difference between sheet and coil RSS surfaces are up to 0.4 ppm ^{1}Hα nuclei (Figure 1c). It is of interest to note that despite of the difference in magnitude, helical and coil RSS surfaces vary similarly with ϕ and ψ for ^{13}Cα, ^{13}CO, and ^{1}Hα nuclei, and therefore the difference between the two surfaces remains almost constant with ϕ and ψ. The same is true for sheet and coil RSS surfaces.

$\langle \Delta\delta(\phi,\psi)_s \rangle$ *and* $\langle \Delta\delta(\phi,\psi)_s \rangle$

To generally evaluate β-sheet and α-helix induced effects on chemical shifts and to further quantitatively describe the variation of such effects with the backbone conformation, the secondary structural effect correction factors, $\Delta\delta(\phi, \psi)_{sheet}$ and $\Delta\delta(\phi, \psi)_{helix}$, are determined and statistically studied. Their averaged values, $\langle \Delta\delta(\phi,\psi)_{helix} \rangle$ and $\langle \Delta\delta(\phi,\psi)_{sheet} \rangle$, together with RMS deviations over each corresponding backbone conformation space are calculated and

Table 1. Secondary structural effect correction factors, $\langle \Delta\delta(\phi,\psi)_{\text{sheet}} \rangle$ and $\langle \Delta\delta(\phi,\psi)_{\text{helix}} \rangle$. In the brackets are the RMS deviations

Amino acids	^{13}CO		^{13}Cα		^{13}Cβ		1Hα		15N		1HN	
	Sheet	Helix	Sheet	Helix	Sheet	Helix	Sheet	Helix	Sheet	Helix	Sheet	Helix
Ala	−0.92(0.35)	1.36(0.10)	−0.65(0.38)	0.90(0.28)	1.23(0.73)	−0.87(0.24)	0.42(0.13)	−0.12(0.04)	0.44(1.42)	0.26(0.35)	0.22(0.11)	0.12(0.08)
Arg	−0.51(0.32)	1.41(0.18)	−0.24(0.33)	1.35(0.37)	1.33(0.43)	−0.41(0.39)	0.37(0.09)	−0.18(0.04)	0.77(1.03)	0.37(0.42)	0.28(0.23)	0.03(0.10)
Asn	−0.63(0.34)	1.63(0.36)	−0.02(0.22)	1.73(0.23)	1.17(0.83)	−0.07(0.19)	0.28(0.12)	−0.15(0.02)	1.29(1.00)	1.03(0.36)	0.16(0.14)	−0.06(0.14)
Asp	−0.47(0.28)	1.62(0.11)	0.18(0.38)	1.54(0.47)	0.63(0.44)	−0.15(0.13)	0.29(0.10)	−0.11(0.06)	1.41(0.97)	1.23(0.37)	0.19(0.16)	−0.08(0.07)
Cys (reduced)	−0.49(0.64)	0.74(0.71)	−0.06(1.06)	1.98(0.70)	3.39(1.97)*	−1.83(2.89)*	0.40(0.35)	−0.29(0.19)	−0.24(1.71)	−1.61(0.91)	0.31(0.35)	0.10(0.23)
Cys (oxidized)	0.13(1.63)	1.32(0.51)	0.79(1.03)	1.94(0.59)	0.43(0.51)	−1.77(1.16)*	0.31(0.14)	−0.15(0.18)	1.81(2.04)	1.48(1.15)	0.27(0.30)	0.20(0.29)
Gln	−0.54(0.24)	1.63(0.18)	−0.18(0.27)	1.12(0.23)	1.27(0.68)	−0.21(0.23)	0.29(0.08)	−0.14(0.04)	0.12(1.38)	0.17(0.34)	0.12(0.23)	−0.04(0.05)
Glu	−0.68(0.23)	1.55(0.17)	−0.42(0.34)	0.92(0.21)	1.67(0.66)	−0.32(0.22)	0.41(0.07)	−0.14(0.04)	0.54(0.97)	0.65(0.43)	0.16(0.22)	−0.06(0.06)
Gly	−0.93(0.67)	1.19(0.34)	−0.08(0.43)	1.04(0.24)			0.12(0.11)	−0.08(0.08)	0.84(1.19)	−0.79(0.74)	0.30(0.14)	−0.16(0.10)
Leu	−0.64(0.31)	1.17(0.26)	−0.24(0.31)	1.14(0.26)	1.41(0.58)	−0.52(0.26)	0.36(0.08)	−0.20(0.05)	0.60(0.61)	−0.05(0.42)	0.39(0.20)	0.33(0.07)
Lys	−0.59(0.27)	1.48(0.22)	−0.33(0.29)	1.07(0.19)	1.31(0.67)	−0.23(0.16)	0.39(0.10)	−0.16(0.03)	0.77(1.00)	0.52(0.34)	0.16(0.16)	0.01(0.15)
Met	−0.34(0.51)	1.32(0.29)	−0.51(0.44)	1.12(0.39)	0.89(0.82)	−0.34(0.29)	0.36(0.10)	−0.22(0.07)	0.62(0.98)	−0.34(0.63)	0.21(0.28)	0.06(0.07)
Ser	−0.58(0.42)	1.02(0.06)	0.02(0.35)	1.49(0.46)	0.58(0.73)	−0.43(0.20)	0.35(0.13)	−0.15(0.06)	0.44(0.75)	0.57(0.51)	0.21(0.20)	0.06(0.08)
Pro	−1.00(0.41)	1.30(0.07)	−0.47(0.27)	1.23(0.26)	0.07(1.11)*	−0.49(0.19)	0.32(0.15)	−0.14(0.04)				
His*	−0.25(0.76)	1.72(0.24)	0.10(0.56)	1.51(0.28)	1.11(0.83)	0.47(0.28)	0.27(0.15)	−0.02(0.09)	0.50(1.38)	1.17(0.85)	0.29(0.37)	−0.08(0.11)
Tyr*	0.09(0.60)	1.11(0.40)	0.27(0.35)	0.53(0.54)	1.25(0.59)	−0.34(0.47)	0.23(0.09)	−0.12(0.06)	0.20(1.41)	−0.26(0.46)	0.52(0.24)	0.09(0.06)
Phe*	−0.63(0.47)	0.85(0.13)	−0.23(0.37)	1.47(0.14)	1.42(0.48)	−0.02(0.25)	0.29(0.08)	−0.14(0.05)	0.17(1.28)	−0.48(0.53)	0.25(0.20)	0.08(0.12)
Trp*	−0.12(0.58)	1.89(0.37)	−0.60(0.89)	1.06(0.34)	1.63(0.77)	−0.44(0.31)	0.26(0.16)	0.03(0.10)	0.05(2.62)	0.27(0.86)	0.22(0.30)	0.46(0.09)
Ile*	−0.31(0.14)	0.88(0.40)	−0.12(0.28)	1.77(0.37)	0.92(0.81)	−0.29(0.32)	0.46(0.07)	−0.28(0.07)	0.05(1.36)	0.32(0.92)	0.43(0.23)	0.34(0.12)
Val*	−0.46(0.20)	0.55(0.15)	−0.53(0.24)	1.43(0.29)	1.01(0.37)	−0.52(0.22)	0.42(0.05)	−0.34(0.04)	0.91(0.95)	−0.96(0.52)	0.34(0.18)	0.19(0.08)
Thr*	−0.37(0.43)	0.96(0.15)	0.35(0.42)	1.63(0.58)	0.14(0.68)	−0.26(0.47)	0.44(0.07)	−0.28(0.06)	2.67(1.28)	1.40(1.75)	0.33(0.27)	0.07(0.04)
Average	**−0.67(0.49)**	**1.27(0.25)**	**−0.29(0.44)**	**1.37(0.39)**	**1.02(0.66)**	**−0.30(0.27)**	**0.36(0.12)**	**−0.17(0.07)**	**0.64(1.27)**	**0.29(0.75)**	**0.28(0.25)**	**0.16(0.11)**

*Data listed in this table are calculated from XRSS surfaces, where the most populated staggered conformations, $\chi^1 = 180 \pm 30°$ for Val; $\chi^1 = -60 \pm 30°$ for Ile, Thr, Phe, His, Tyr, and Trp are used. The results from all the three staggered conformations agree well to each other except for those with no sufficient data for statistical analysis.

listed in Table 1. Of the importance in deciphering β-sheet and α-helix-induced changes in ^{13}CO, $^{13}C\alpha$, $^{13}C_\beta$, $^{1}H\alpha$, ^{15}N, and ^{1}HN chemical shifts, this table reveals the following:

First, β-sheet and α-helix induced changes in $^{13}C\alpha$, ^{13}CO, and $^{1}H\alpha$ chemical shifts vary little with the backbone conformation (ϕ and ψ) for all the 20 amino acids. This is characterized by the small RMS deviations of $\Delta\delta(\phi, \psi)_s$ over helix ($\phi = -40$ to $-100°$; $\psi = -10$ to $-70°$) and β-sheet ($\phi = -50$ to $-180°$; $\psi = 80$ to $180°$) conformational spaces. Averaging over all the 20 amino acids, the RMS deviations of $\Delta\delta(\phi, \psi)_{sheet}$ are 0.49, 0.44, and 0.39 ppm for $^{13}C\alpha$, ^{13}CO and $^{1}H\alpha$ nuclei, respectively; those of $\Delta\delta(\phi, \psi)_{helix}$ are 0.25, 0.39, and 0.07 ppm. On the other hand, the variations of $\Delta\delta(\phi, \psi)_{sheet}$ and $\Delta\delta(\phi, \psi)_{helix}$ with ϕ and ψ are significantly larger for ^{15}N and ^{1}HN nuclei. On average, RMS deviations of $\Delta\delta(\phi, \psi)_{sheet}$ are up to 1.27 ppm and 0.75 ppm for ^{15}N and ^{1}HN, respectively; and those of $\Delta\delta(\phi, \psi)_{helix}$ are 0.75 ppm and 0.11 ppm.

Second, the averaged secondary structural effect correction factors, $\Delta\delta(\phi,\psi)_{helix}\rangle$ and $\langle\Delta\delta(\phi,\psi)_{sheet}\rangle$ vary little with the 20 amino acids. The averaged values and RMS deviations of $\langle\Delta\delta(\phi,\psi)_{sheet}\rangle$ over the 20 amino acids are: −0.67(0.25), −0.29(0.25), 1.02(0.66), 0.36(0.09), 0.64 (0.43), and 0.28(0.11) for $^{13}C\alpha$, ^{13}CO, $^{13}C\alpha$, $^{1}H\alpha$, ^{15}N, and ^{1}HN nuclei, respectively; those of $\langle\Delta\delta(\phi,\psi)_{helix}\rangle$ are 1.27(0.38), 1.37(0.35), −0.39 (0.27), −0.17(0.10), 0.29(0.77), and 0.16(0.22). Notable exceptions are $\langle\Delta\delta(\phi,\psi)_{helix}\rangle$, as indicated by their large RMS deviations, 0.77 and 0.22, for ^{15}N, and ^{1}HN nuclei, respectively. Close inspection on the data in Table 1 reveals that: helical effect on ^{1}HN shifts can be related to the side-chain property of the 20 amino acids. For example, the values of $\langle\Delta\delta(\phi,\psi)_{helix}\rangle$ for ^{1}HN are negative for amino acids with short and chargeable side chains that include Asn, Asp, Cys, Gln, Glu, and His; while that for all other amino acids are positive. Meanwhile, the values of $\langle\Delta\delta(\phi,\psi)_{helix}\rangle$ for amino acid Gly's ^{1}HN and ^{15}N shifts are distinguishable from that of other 19 amino acids. These unusual $\langle\Delta\delta(\phi,\psi)_{helix}\rangle$ values could possibly be attributed to the special conformation formed by these amino acids. For example, Asp, Asn, and Cys have preference to form helical capping box (Aurora and Rose, 1998), and Gly is often located at the end of α-helix.

Third, due to the different definitions, the present secondary structural effect correction factors, $\langle\Delta\delta(\phi,\psi)_{helix}\rangle$ and $\langle\Delta\delta(\phi,\psi)_{helix}\rangle$, are significantly smaller in magnitude than those reported in earlier studies. Over the past 20 years, the secondary structural effects on chemical shifts in proteins have been investigated through comparing the observed β-sheet or α-helix chemical shifts with an set of 'random-coil' chemical shifts, which is usually obtained either by measuring the chemical shifts of model peptide in denaturing conditions or by statistically averaging the assigned chemical shift for amino acids at coil status. In this study, the RSS shielding surfaces were used to investigate the secondary structural effects on chemical shifts in proteins. More specifically, the β-sheet induced effects are quantitatively determined by comparing the β-sheet specific RSS surfaces with the random-coil specific RSS surfaces. Similarly, α-helix induced effects were studied by comparing α-helix specific RSS surfaces with random-coil RSS surfaces. As a consequence, the proposed secondary structural effect differs from the traditional definition by separating out the backbone conformational effects.

To quantitatively evaluate this difference, the secondary structural effect correction factors recently reported by Wang and Jardetzky (2002b) were chosen to compare with the present results. The two sets of data (both were averaged over the 20 amino acids for simplicity) were graphically displayed in Figure 2. More specifically, the present β-sheet correction factors are 48%, 83%, 47%, 21%, 67%, and 41% less in magnitude than those by Wang and Jardetzky for ^{13}CO, $^{13}C\alpha$, $^{13}C_\beta$, $^{1}H\alpha$, ^{15}N, and ^{1}HN shifts, respectively. For α-helix induced effects, the present results are 35%, 56%, and 49% less than the earlier values for ^{13}CO, $^{13}C\alpha$, and $^{1}H\alpha$ shifts, respectively. Since the a-helix induced effects are very small for $^{13}C_\beta$, ^{15}N and ^{1}HN, no comparisons were made for these three nuclei.

$\Delta\delta^{pre\text{-}obs}$ and chemical shift prediction using RSS

Predicting chemical shifts from known structure is an important step toward understanding the relation between chemical shifts and protein structure. To date, several fundamentally different

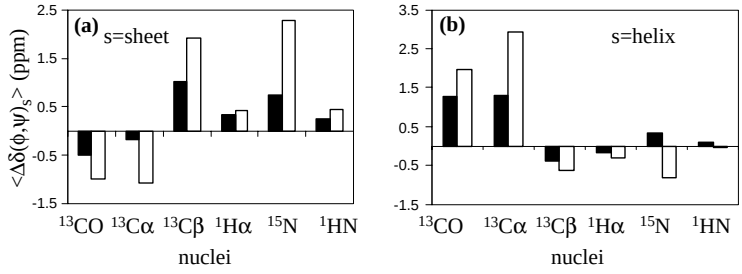

Figure 2. Comparison of the present (solid bar) secondary structural effect correction factors, $\langle \Delta\delta(\phi,\psi)_s \rangle$ and $\langle \Delta\delta(\phi,\psi)_s \rangle$, with that recently reported (open bar) by Wang and Jardetzky (2002b).

techniques have been developed for this purpose. Among these techniques, the empirical ϕ/ψ shielding surface is probably the most practical approach, and allows ^{1}H, ^{13}C, and ^{15}N shifts to be predicted with reasonable accuracy (Le and Oldfield, 1994; Wishart and Nip, 1998; Wang and Jardetzky, 2004). Since the traditional ϕ/ψ shielding surfaces use chemical shifts without distinction of their secondary structural types, the secondary structural effects could be ignored or inappropriately implemented during the chemical shift prediction. To quantitatively evaluate how the secondary structural effects proposed in this study will affect the chemical shift prediction, the status of an amino acid in protein was classified into four categories, sheet, c_sheet, c_helix, and helix (see method section). For each category of data, $\Delta\delta^{\text{pre-obs}}$ of the chemical shifts predicted from non-RSS surfaces were theoretically estimated using the secondary structural effect correction factors, $\langle \delta(\phi,\psi)_{\text{helix}} \rangle$ and $\langle \Delta\delta(\phi,\psi)_{\text{sheet}} \rangle$. Table 2 lists the estimated $\Delta\delta^{\text{pre-obs}}$ values of ^{13}Cα, ^{13}CO, and ^{1}Hα shifts from non-RSS surfaces. As shown in this table, the $\Delta\delta^{\text{pre-obs}}$ values for non-RSS surfaces show different trend between the four categories of data, sheet, c_sheet, c_helix, and helix. Three significantly large $\Delta\delta^{\text{pre-obs}}$ values were identified and highlighted in Table 2. Specifically, $\Delta\delta^{\text{pre-obs}}$(c_helix) are 1.05 ppm and 1.13 ppm for ^{13}CO and ^{13}Cα shifts, respectively; $\Delta\delta^{\text{pre-obs}}$ (c_sheet) 0.23 ppm for ^{1}Hα shifts. Also given in Table 2 are the occurrence probabilities for an amino acid in proteins to be classified into each of the four categories. Therefore, the data shown in Table 2 gives a clear view of how chemical shifts predicted from non-RSS surfaces deviate from the observed values. For example, the occurrence probability of helix-like coil is 7%, which indicates the same percentage of ^{13}CO and ^{13}Cα shifts predicted using non-RSS would unavoidably differ by more than 1.0 ppm from the observed values. Similarly, those β-sheet-like random-coil shifts, which have the occurrence probability of 13%, will deviate by around 0.20 ppm from the observed values.

To determine the accuracy of the theoretical values of $\Delta\delta^{\text{pre-obs}}$ listed in Table 2, 1000 chemical shift entries were randomly selected from the database for each ^{13}Cα, ^{13}CO, and ^{1}Hα nuclei, and their chemical shifts were predicted using non-RSS and RSS surfaces. The predicted chemical shifts were grouped into categories of sheet, c-sheet, c_helix, and helix; and $\Delta\delta^{\text{pre-obs}}$ were calculated and graphically displayed in Figure 3. For comparison, the theoretically calculated $\Delta\delta^{\text{pre-obs}}$ values in Table 2 are also shown in this figure. For non-RSS surfaces, the two sets of $\Delta\delta^{\text{pre-obs}}$, theoretical values listed in Table 2 and those calculated from the testing data, were in a very good agreement. In the other hand, $\Delta\delta^{\text{pre-obs}}$ for chemical shifts predicted using RSS were

Table 2. Theoretically calculated $\Delta\delta^{\text{pre-obs}}$ (in ppm) of the ^{13}CO, ^{13}Cα, and ^{1}Hα chemical shifts predicted from non-RSS surfaces

	^{13}CO	^{13}Cα	1Hα	Occurrence (%)*
$\Delta\delta^{\text{pre-obs}}$ (sheet)	0.23	0.1	−0.13	24
$\Delta\delta^{\text{pre-obs}}$ (c_sheet)	−0.44	−0.19	**0.23**	13
$\Delta\delta^{\text{pre-obs}}$ (c_helix)	**1.05**	1.13	−0.14	7
$\Delta\delta^{\text{pre-obs}}$ (helix)	−0.22	−0.24	0.03	31

*The probability for an amino acid to be in the corresponding category. 29% of the data, which does not belong to any of the four groups, is composed by β-sheet (2.5%), coil (24.4%), and α-helix (3.1%).

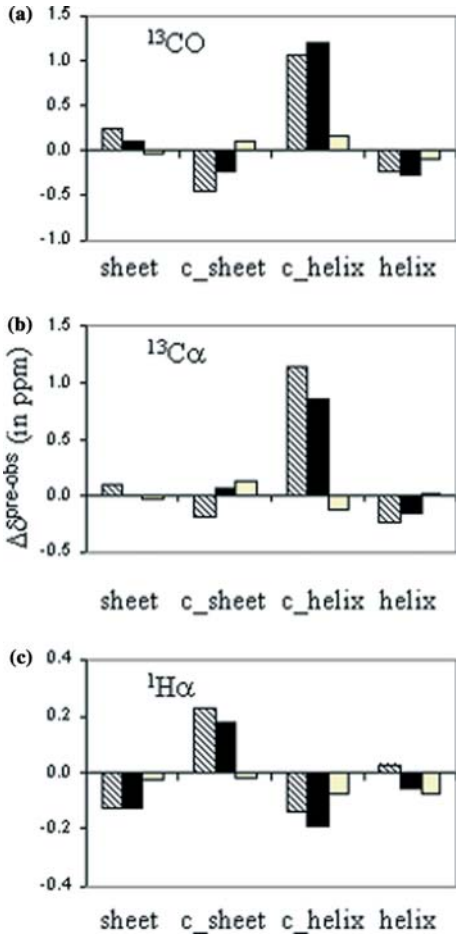

Figure 3. $\Delta\delta^{pre\text{-}obs}$ of ^{13}CO (a), ^{13}Cα (b), and ^{1}Hα (c) chemical shifts predicted using non-RSS (solid bar) and RSS (open bar) surface. For comparison, the theoretically calculated $\Delta\delta^{pre\text{-}obs}$ values are shown by the shallow bar.

found to be insignificant for all the four categories of data, sheet, c_sheet, c_helix, and helix.

The present RSS shielding surfaces simultaneously take into account the backbone conformational effects and secondary structural effects in predicting chemical shifts in protein. To further assess the efficiency of RSS shielding surfaces, 300 ^{13}Cα, ^{13}CO, ^{15}N, ^{1}Hα, and ^{1}HN chemical shift entries were randomly selected for each of the 20 amino acids and used for testing. Chemical shift predictions for each selected entry were made using RSS and non-RSS shielding surfaces. Two parameters, RMS deviation and the correlation coefficient of linear regression fits between the observed and the predicted chemical shifts, are used for the evaluation. Based on the above analysis, RSS will improve the prediction of the β-sheet like coil shifts for ^{13}CO and ^{13}Cα, and α-helix like coil shifts for ^{1}Hα nuclei.

From non-RSS to RSS shielding surfaces, modestly improved predictions on ^{13}Cα, ^{13}CO, and ^{1}Hα shifts are demonstrated by the increased correlation coefficients and decreased RMS deviations for all the 20 amino acids. On average, the correlation coefficients are 0.66 0.80, and 0.68 for ^{13}Cα, ^{13}CO, and ^{1}Hα shifts predicted from non-RSS; and those from RSS surfaces are 0.68, 0.81, and 0. 71. The rmsd values are 1.37, 1.30, 0.36 for ^{13}Cα, ^{13}Cα, and ^{1}Hα shifts predicted from non-RSS; and those from RSS surfaces are 1.33, 1.28, and 0.34. The overall improvements in the prediction of ^{13}CO, ^{13}Cα and ^{1}Hα shifts from non-RSS to RSS are not remarkable. This is due to that fact that the occurrence probability of β-sheet and α-helix like coils are not high (7% and 13%, respectively). As shown Table 1, the secondary structural effects on $^{13}C_{\beta}$, ^{15}N, and ^{1}HN chemical shifts are relatively smaller than that on the other three nuclei. As a consequence, from non-RSS to RSS shielding surfaces, the improvements on the prediction of ^{15}N and ^{1}HN shifts are not obvious.

Comparison with other approaches

Three programs that can automatically predict protein chemical shifts from its 3D coordinates have been recently published. They are SHIFTS, which uses density functional theory (Xu and Case, 2001, 2002), SHIFTX, which is based on a hybrid predictive approach (Neal et al., 2003), and PROSHIFTS, which is based on a neural network (Meiler, 2003). Thirteen proteins (eight were selected from present database, and five are newly released BMRB entries) were chosen and their ^{13}CO, ^{13}Cα, and ^{1}Hα chemical shifts were predicted using the present RSS (and XRSS), SHIFTX (version 1.0; http://redpoll.pharmacy.ualberta.ca), SHIFTS (version 4.1; http://www.scripps.edu/case), and PROSHIFT (current version, http://www.jens-meiler.de).

Performance evaluations for the four programs were made by comparison of the observed shifts with those predicted by each program. The correlation coefficients, averaged deviations, and RMS deviations between the observed ^{13}Cα chemical shifts and those predicted for the testing

Table 3. Correlation coefficients, averaged and RMS deviations for linear regression fits of the observed $^{13}C\alpha$ chemical shifts versus those predicted using RSS, SHIFTX[a], SHIFTS[b], and PROSHIFT[c] for the thirteen testing proteins

Proteins (BMRB & PDB #)	Correlation coefficients				Averaged deviation				RMS deviation			
	RSS	SHIFTX	SHIFTS	PROSHIFT	RSS	SHIFTX	SHIFTS	PROSHIFT	RSS	SHIFTX	SHIFTS	PROSHIFT
FimC (4070, 1QUN)	0.96	0.96	0.93	0.94	−0.05	−0.24	−0.20	1.70	1.13	1.19	1.60	1.38
NNOS PDZ (4304, 1B8Q)	0.97	0.96	0.94	0.97	−0.02	−0.40	−0.14	1.76	1.29	1.47	1.77	1.18
Bet v 1-L (4417, 1B6F)	0.97	0.97	0.95	0.97	0.04	−0.26	0.03	1.67	1.26	1.28	1.58	1.20
Apaf_1 CARD (4661, 2YGS)	0.97	0.98	0.96	0.96	0.02	0.04	−0.05	1.94	1.03	0.89	1.18	1.16
Ub1D8 (4663, 1C3T)	0.97	0.97	0.95	0.97	−0.03	−0.24	−0.28	1.69	1.10	1.10	1.37	1.07
HEDA (5027, 1J8K)	0.96	0.95	0.93	0.97	−0.14	−0.15	0.05	1.69	1.24	1.57	1.85	1.12
MTP 1598 (5165, 1JW3)	0.97	0.95	0.93	0.97	0.00	−0.08	0.05	1.74	1.08	1.37	1.67	1.19
RRF (5190, 1EK8)	0.98	0.98	0.96	0.98	−0.06	−0.16	−0.05	1.96	0.93	0.97	1.31	0.97
a_ADT (5936, 1E0R)	0.97	0.95	0.92	0.94	0.03	−0.17	−0.09	1.81	1.15	1.35	1.74	1.50
HIV-1 Rnase (5931, 1HRH)	0.97	0.97	0.97	*0.88*	0.05	−0.13	−0.02	1.71	1.30	1.31	1.28	*2.55**
PSP (5799, 1F5S)	0.97	0.98	0.97	0.97	0.09	−0.01	0.04	1.90	1.13	0.98	1.28	1.18
CD44 (6093, 1POZ)	0.95	0.93	0.91	0.93	0.06	−0.27	0.04	1.74	1.45	1.74	1.93	1.71
BstL18 (5970, 1OVY)	0.96	0.94	0.92	0.95	0.09	−0.24	−0.35	1.77	1.38	1.67	1.84	1.42
Average	**0.97**	**0.96**	**0.94**	**0.96**	**0.01**	**−0.18**	**−0.07**	**1.78**	**1.19**	**1.30**	**1.57**	**1.26**
(standard deviation)	**(0.01)**	**(0.02)**	**(0.02)**	**(0.03)**	**(0.07)**	**(0.12)**	**(0.13)**	**(0.10)**	**(0.15)**	**(0.27)**	**(0.26)**	**(0.21)**

*This extremely large value is not included in the calculation of average and standard deviation.
[a]SHIFTX – version 1.0 (Neal et al., 2003).
[b]SHIFTS – version 4.1 (Xu and Case, 2001, 2002); side-chain refinements were applied during the prediction.
[c]PROSHIFT – current version (Meiler, 2003).

proteins are listed in Table 3. PROSHIFTS gives extremely large deviations for ^{13}C shifts – 1.87 ppm for ^{13}CO and 1.77 ppm for $^{13}C\alpha$ nuclei. This is due to the fact that this program uses TMS rather than DSS or TSP as the ^{13}C chemical shift reference. The difference between TMS and DSS or TSP is around 1.7 ppm (Wishart et al., 1995). Effectively, there is no statistically significant difference for the results shown in Table 3 between the four programs SHIFTS, SHIFTX, PROSHIFT, and RSS. The RSS and XRSS shielding surface takes three parameters: backbone conformation, secondary structural effects, and χ_1 effects (for amino acids Val, Ile, Thr, Phe, His, Tyr, and Trp) in predicting ^{13}CO, $^{13}C\alpha$, and $^{1}H\alpha$ shifts in proteins. Better prediction using present RSS shielding surfaces could be reached by taking into account additional parameters used by the three other programs, which includes aromatic ring effects, hydrogen-bond, and solvent effect, etc.

In addition, it is of interest to know if the secondary structural effects are taken into account in chemical shift prediction by the other three programs, SHIFTX, SHIFTS, and PROSHIFT. To investigate this, $\Delta\delta^{\text{pre-obs}}$(sheet), $\Delta\delta^{\text{pre-obs}}$ (c_sheet), $\Delta\delta^{\text{pre-obs}}$ (c_helix), and $\Delta\delta^{\text{pre-obs}}$ (helix) were calculated for the thirteen testing proteins with each program. The results are listed in Table 4. The omission of secondary structural effects by SHIFTX and SHIFTS are directly evidenced by their large $\Delta\delta^{\text{pre-obs}}$ (c_helix) – 1.20 ppm and 1.08 ppm (*versus* the theoretical value of 1.13 in Table 2) for $^{13}C\alpha$ shifts; 0.96 ppm and 1.64 ppm (*versus* 1.05 ppm in Table 2) for ^{13}CO shifts. Since PROSHIFT uses TMS as the ^{13}C chemical shift reference, reference correction adjustment was made by adding

Table 4. $\Delta\delta^{pre\text{-}obs}$ (in ppm) for ^{13}CO, $^{13}C\alpha$, and $^{1}H\alpha$, chemical shifts predicted using SHIFTX, SHIFTS, and PROSHIFT

Nuclei	$\Delta\delta^{pre\text{-}obs}$	SHIFTX	SHIFTS	PROSHIFT*
^{13}CO	$\Delta\delta_{sheet}$	−0.16	0.11	0.42
	$\Delta\delta_{c\_sheet}$	−0.15	−0.49	−0.15
	$\Delta\delta_{c\_helix}$	**0.96**	**1.64**	**0.52**
	$\Delta\delta_{helix}$	0.01	−0.08	−0.48
$^{13}C\alpha$	$\Delta\delta_{sheet}$	0.22	0.17	0.18
	$\Delta\delta_{c\_sheet}$	−0.01	−0.1	0.15
	$\Delta\delta_{c\_helix}$	**1.2**	**1.08**	**0.44**
	$\Delta\delta_{helix}$	−0.01	−0.09	−0.21
$^{1}H\alpha$	$\Delta\delta_{sheet}$	**−0.10**	–	**−0.11**
	$\Delta\delta_{c\_sheet}$	−0.03	–	0.04
	$\Delta\delta_{c\_helix}$	−0.12	–	−0.01
	$\Delta\delta_{helix}$	0.06	–	0.09

*Reference correction adjustment was made by adding 1.7 ppm to ^{13}CO and $^{13}C\alpha$ shifts predicted by PROSHIFT.

1.7 ppm to the ^{13}C shifts predicted by this program. After the ^{13}C chemical shift correction, $\Delta\delta^{pre\text{-}obs}$ (c_helix) of PROSHIFT are 0.44 ppm and 0.52 ppm for $^{13}C\alpha$ and ^{13}CO shifts. These values follow the same trend but are smaller than those in Table 2. Meanwhile, $\Delta\delta^{pre\text{-}obs}$ (sheet) and $\Delta\delta^{pre\text{-}obs}$ (helix) of $^{1}H\alpha$ shift from PROSHIFT are −0.11 and 0.09 ppm, respectively, resulting a net difference of up to 0.2 ppm. These data indicate that the secondary structural effects might not be adequately considered by this program.

Conclusion

This study presents a new definition of the secondary structural effect on protein chemical shifts. By separating out the backbone conformational effects, the values differ from and are significantly smaller than those reported in earlier studies. The proposed new concept provided by the definition gives insight into the understanding and the origins of observed chemical shifts. This paper also identifies unexpected shortcomings of the traditional ϕ/ψ shielding surfaces as well as other chemical shift prediction programs: depending on the ϕ/ψ dihedral angles and secondary status, the predicted chemical shifts systematically deviate from the observed values. Such systematic deviations are significant, e.g., above 1.0 ppm for α-helix like random coil ^{13}C shifts, and can be avoided by using the chemical shifts database with distinction of their secondary structural types.

Acknowledgements

The author would like to thank both the reviewers for their advices, specifically for one of the reviewers for his suggestion of using the nomenclature of 'Residue-specific Secondary Structure Shielding Surface (RSS)'. The author also wishes to acknowledge Ms. Natasha Lavelle for her help in proofreading the manuscript.

Supporting Information Available: One table containing the BMRB and PDB accession numbers access of the proteins used in this study. Available free of charge via the Internet at http://kluweronline.com/issn/0925–2738

References

Aurora, R. and Rose, G.D. (1998) *Protein Sci.,* **7**, 21–38.
Beger, R.D. and Bolton, P.H. (1997) *J. Biomol. NMR*, **10**, 129–142.
Celda, B., Biamonti, C., Arnau, M.J., Tejero, R. and Montelione, G.T. (1995) *J. Biomol. NMR*, **5**, 161–172.
Cornilescu, G., Delaglio, F. and Bax, A. (1999) *J. Biomol. NMR*, **13**, 289–302.
de Dios, A.C., Pearson, J.G. and Oldfield, E. (1993) *Science*, **260**, 1491–1495.
Iwadate, M., Asakura, T. and Williamson, M.P. (1999) *J. Biomol. NMR*, **13**, 199–211.
Kuszewski, J., Gronenborn, A.M. and Clore, G.M. (1995) *J. Magn. Reson.,* **B 107**, 293–297.
Le, H. and Oldfield, E. (1994) *J. Biomol. NMR*, **4**, 341–348.
Markley, J.L., Meadows, D.H. and Jardetzky, O. (1967) *J. Mol. Biol.*, **27**, 25–40.
Meiler, J. (2003) *J. Biomol. NMR,* **26**, 25–37.
Nakamura, A. and Jardetzky, O. (1968) *Biochemistry*, **7**, 1226–1230.
Neal, S., Nip, A.M., Zhang, H. and Wishart, D.S. (2003) *J. Biomol. NMR*, **26**, 215–240.
Oldfield, E. (1995) *J. Biomol. NMR,* **5**, 217–225.
Osapay, K. and Case, D.A. (1994) *J. Biomol. NMR*, **4**, 215–230.
Roberts, G.C. and Jardetzky, O. (1970) *Adv. Protein Chem.,* **24**, 447–545.
Spera, S. and Bax, A. (1991) *J. Am. Chem. Soc.*, **113**, 5490–5492.

Szilagyi, L. and Jardetzky, O. (1989) *J. Magn. Reson.*, **83**, 441–449.
Wang, Y. and Jardetzky, O. (2002a) *Protein Sci.*, **11**, 852–861.
Wang, Y. and Jardetzky, O. (2002b) *J. Am. Chem. Soc.*, **124**, 14075–14084.
Wang, Y. and Jardetzky, O. (2004) *J. Biomol. NMR*, **28**, 327–340.
Willard, L., Ranjan, A., Zhang, H., Monzavi, H., Boyko, R.F., Sykes, B.D. and Wishart, D.S. (2003) *Nucl. Acids Res.,* **31**, 3316–3319.
Williamson, M.P., Kikuchi, J. and Asakura, T. (1995) *J. Mol. Biol.,* **247**, 541–546.
Wishart, D.S. and Case, D.A. (2001). *Meth. Enzymol.*, **338**, 3–34.
Wishart, D.S. and Nip, A.M. (1998) *Biochem. Cell Biol.*, **76**, 1–10.
Wishart, D.S. and Sykes, B.D. (1994) *J. Biomol. NMR,* **4**, 171–180.
Wishart, D.S., Bigam, C.G., Holm, A., Hodges, R.S. and Sykes, B.D. (1995) *J. Biomol. NMR*, **5**, 67–81.
Wishart, D.S., Sykes, B.D. and Richards, F.M. (1991) *J. Mol. Biol.*, **222**, 311–333.
Wishart, D.S., Sykes, B.D. and Richards, F.M. (1992) *Biochemistry,* **31**, 1647–1651.
Xu, X-P. and Case, D.A. (2001) *J. Biomol. NMR*, **21**, 321–333.
Xu, X-P. and Case, D.A. (2002) *Biopolmers*, **65**, 215–240.
Zhang, H., Neal, S. and Wishart, D.S. (2003) *J. Biomol. NMR*, **25**, 173–195.